

# Prokaryotic Expression of Active Mitochondrial Uncoupling Protein 1\*

ZHOU Qiang-Jun, SUN Ji, ZHAI Yu-Jia, SUN Fei\*\*

(National Laboratory of Biomacromolecules, Institute of Biophysics, The Chinese Academy of Sciences, Beijing 100101, China)

**Abstract** Mitochondrial respiratory oxidation is coupled with ATP synthesis. This coupling process can be broken by uncoupling protein (UCP), an integral membrane protein at mitochondrial inner membrane. Here, active rat UCP1 (rUCP1) was expressed in *E. coli*. Expression of rUCP1 can lower host's growth rate. Immuno-electron microscopy proved expressed rUCP1 was mainly located on membrane. Purified rUCP1 was reconstituted into liposome and exhibited proton translocation activity. These results revealed eukaryotic UCP1 could be expressed in active form by prokaryotes and enable us to obtain enough amount of rUCP1 for structural study.

**Key words** mitochondrial uncoupling protein, prokaryotic expression, immune-electron microscopy, membrane protein, liposome

**DOI:** 10.3724/SP.J.1206.2009.00531

As the important “energy factory” of eukaryotic cell, mitochondrion is the place for cellular respiration *via* oxidative phosphorylation process (OXPHOS). OXPHOS electron transfer chain is located at the inner membrane of mitochondrion and comprising of four large trans-membrane protein complexes as well as ubiquinone and cytochrome *c*. The function of mitochondrial respiration chain is to transfer electron from NADH/FADH<sub>2</sub> to oxygen and simultaneously pump proton from matrix to inter-membrane space. This oxidation process is coupled with phosphorylation process where ATP synthesis enzyme (ATPase, called Complex V) uses the proton gradient energy across inner membrane to produce ATP molecule. The couple between oxidation and phosphorylation could be dissipated by uncoupling proteins (UCPs) located in the inner membrane. Proton from the inter-membrane space will go *via* UCP back to matrix producing heat instead of ATP.

UCPs(31~34 ku) belong to mitochondrial anion-carrier protein super-family and can be classified into five homologues UCP1, UCP2, UCP3, UCP4 and UCP5<sup>[1-2]</sup>. UCP1 is classically associated with the non-shivering thermogenesis of brown adipose tissue (BAT) from newborns, cold acclimatized and hibernating mammals, and overfed rodents<sup>[3]</sup>. The proton translocation activity of UCP1 could be

inhibited by purine nucleotides (ATP, ADP, GTP and GDP)<sup>[4-5]</sup> and activated by fat acid (FA)<sup>[6-8]</sup>. There are two models under debate for the proton translocation mechanism of UCP1: “proton-buffering model” and “fatty acid cycling model”. In the first model, proton would be directly transported from inter-membrane space to matrix *via* the channel in UCP1. However, in the second model, UCP1 was considered as the translocase of fatty acyl anions from matrix to inter-membrane space. Fatty acyl anions will accept proton in inter-membrane space and become free fatty acids that can flip-flop across the inner membrane back into matrix and release proton<sup>[2]</sup>. Besides UCP1, UCP2 and UCP3 are well studied however their physiological functions are not entirely clear but believed to be related with reactive oxygen species (ROS) production and type-2 diabetes. Therefore, the atomic structures of UCPs are very important for understanding its molecular mechanism as well as the therapy of related diseases.

\*This work was supported by grants from National Basic Research Program of China (2006CB503910, 2006CB806506, 2006CB911001) and The National Natural Science Foundation of China (30721003).

\*\*Corresponding author.

Tel: 86-10-64888582, E-mail: feisun@ibp.ac.cn

Received: September 10, 2009 Accepted: December 1, 2009

There is still no 3D structure available in UCP family besides it is known that UCPs are comprised of three repeats and each repeat contains two trans-membrane helixes and the loops between these trans-membrane helixes take important function for UCPs' transporter activity. The functional form of UCPs was proposed as a dimer<sup>[2-9]</sup>. Within mitochondrial anion-carrier protein super-family, there is one membrane protein ATP/ADP carrier whose crystal structure was solved<sup>[10]</sup> and believed to share same fold with UCPs.

Due to the importance of UCP1, researchers have tried many methods to purify this 32 ku membrane protein. UCP1 can be purified directly from BAT<sup>[11-12]</sup> with abundance of detergent (Triton X-100) that is not feasible for further structure study. And UCP1 could be expressed in *E. coli* and purified from inclusion bodies<sup>[13]</sup>. Yeast expression system was also used to express UCP1 and UCP3 without large-scale purification<sup>[14-15]</sup>.

Here we report our observation of expressing rat UCP1 (rUCP1) in *E. coli*. The growth rate of those *E. coli* strains that express rUCP1 is significantly lower than the control strains, indicating the expressed rUCP1 can greatly inhibit the growth of *E. coli*. And the expressed rUCP1 was found to be significantly located on the cell membrane of *E. coli* by immune-electron microscopy. Recombinant rUCP1 was purified and reconstituted into liposome and found to have clear proton translocation activity. Those results revealed, UCP1, a eukaryotic six-trans-membrane protein, could be expressed by *E. coli* in its active form. This observation enables us to do large scale expression and purification for further structural study.

## 1 Materials and methods

### 1.1 Cloning, expression and purification of rUCP1

The cDNA of rUCP1 (*Rattus norvegicus*) was a gift from Prof. Zhang C.Y. (National Pharmaceutical & Medical Key Laboratory, School of Life Science, Nanjing University).

Forward Primer (5' CGG AAT TCG ATG GTG AGT TCG ACA ACT TCC 3') and reverse one (5' ACG CGT CGA CTG TGG TGC AGT CCA CTG TCT G 3') were used to amplify the rUCP1 gene that was finally inserted into the vector pET22b (Novagen). Plasmids were then transformed into *E. coli* strain C41 (DE3) (Novagen). The positive clone was cultured in TB medium<sup>[16]</sup> till  $A_{600}$  reached 1.6 ~ 2.0 and then

0.15 mmol/L IPTG was added to induce the expression of rUCP1 for about 16 h in 16°C.

Cells were harvested and lysed by sonication. After centrifugation at 14 000 r/min (23 708 *g*, Avanti J-26XP, Beckman Coulter) for 30 min, the supernatant was ultra-centrifuged at 35 000 r/min (rotor Ti-45, Optima L-100, Beckman Coulter) for 1 h. The pellet (membrane of *E. coli*) was then resuspended and homogenized with 300 mmol/L NaCl, 10%(v/v) glycerol and 50 mmol/L Tris (pH 8.0). After 2% LDAO (n-dodecyl-N, N-dimethylamine-N-oxide) was added for membrane solubilization, the mixture was stirring on ice for 30 min. The solution was ultra-centrifuged at 35 000 r/min (rotor Ti-45, Optima L-100, Beckman Coulter) for 30 min and the sediment was discarded. The supernatant was then applied to Ni-NTA column (GE Healthcare). After washing by 40 mmol/L imidazole, 0.1% LDAO, 300 mmol/L NaCl, 10%(v/v) glycerol and 50 mmol/L Tris (pH 8.0), rUCP1 was eluted by 200 mmol/L imidazole. The eluted sample was concentrated by ultra-filtration (Millipore) and then applied to Sephadex G25 (GE Healthcare) for purification with the buffer 25 mmol/L Hepes(pH 7.5), 150 mmol/L NaCl, 10% glycerol and 0.1% LDAO.

### 1.2 Bacterial growth curve measurement

Bacteria with the plasmid pET22b, pET22b-LspA (lipoprotein signal peptidase of *E. coli*) or pET22b-rUCP1 transformed were picked up from LB plates into 50 ml TB media and grew into  $A_{600}$  around 0.5. The bacteria concentrations were carefully measured by  $A_{600}$  and used to make equal amount of bacteria cell that were added into a fresh 250 ml TB media. Then all bacteria will begin to grow from the same concentration. The  $A_{600}$  of new cultures were measured every hour. After 6 h growth, the cultured bacteria were transferred to 16°C. After 1 h, IPTG was added to the cultures with the final concentration 0.2 mmol/L to induce target protein expression. Finally, we got the growth curve of *E. coli* strain C41 (DE3) with or without rUCP1 expressed. These experiments were repeated 4 times.

### 1.3 Western blot

After separated by 12% SDS-PAGE, proteins were transferred to a nitrocellulose membrane for 70 min at 300 mA. The primary antibody is Monoclonal Anti-polyHistidine (SigmaH1029) with a working dilution of 1 : 1 000 and the secondary antibody is Peroxidase-Conjugated AffiniPure Goat Anti-Mouse IgG (ZSGB-BIO, ZB-2305) with a working dilution of

1 : 2 500. The membrane was then incubated in Western Blotting Luminol Reagent (SANTA CRUZ BIOTECHNOLOGY, INC sc-2048) and exposed to film.

#### 1.4 Immuno-electron microscopy

In order to investigate the location (membrane or cytoplasm) of the expressed rUCP1 in *E. coli*, immune-electron microscopy was used. The whole protocol is almost same as reported before<sup>[17]</sup>. Briefly, 5 ml C41 (DE3) cells ( $A_{600} \approx 2$ ) were harvested by centrifuging at 6 000 r/min for 3 min and the supernatant was discarded. After washed with 40 mmol/L phosphate buffer (pH 6.8), the pellet was fixed overnight in fixative buffer, 8% (*m/v*) paraformaldehyde, 80 mmol/L potassium phosphate (pH 6.8), 0.75 mol/L Sorbitol, 0.2% (*v/v*) glutaraldehyde. After washed again by phosphate buffer, the pellet was dehydrated in a gradient series of 30%, 50%, 70%, 95% and 100% ethanol (each 10~15 min) and infiltrated by 1 : 1 and 2 : 1 LR-White (Electron Microscopy Sciences)-ethanol (each for 1 h) and finally by 100% LR-White overnight. At last, LR-White was refreshed for further 6 hours' infiltration. All of the above processes were carried on at room temperature. Finally, the resin was polymerized at  $(60 \pm 1)^\circ\text{C}$  for 48 h. Ultra-thin sections were made by ultra-microtome (Leica UC6) and 70 nm sections were picked out and placed onto Formvar-coated nickel grids for further immuno-labeling.

The grids were washed with PBS buffer for 4 times, each for 2 min, and then were blocked by 5% BSA in PBS for 15 min. Then grids were applied 1 h by Anti-His antibody (Sigma) that was diluted 1 : 100 in 5% BSA. After grids were washed twice with 5% BSA, each for 2 min, they were treated for 1 h with Protein A colloidal gold (10 nm, Electron Microscopy Sciences) which was diluted 1 : 2 in 5% BSA. Then grids were washed with 4 drops of PBS and 6 drops of ddH<sub>2</sub>O. The sections were contrasted by 3% aqueous uranyl acetate for 8 min and observed under transmission electron microscope (FEI Tecnai 20) operated at 120 kV. All above steps were carried under room temperature.

#### 1.5 Reconstitution of rUCP1 into liposome and its proton translocation activity

Purified rUCP1 was reconstituted into liposomal membrane by detergent removal technique as reported by Echtay *et al.*<sup>[18]</sup> and Rigaud *et al.*<sup>[19]</sup> In brief, L- $\alpha$ -phosphatidylcholine (Sigma, type XVI-E) along with 4.2% cardiolipin(Avanti) and 1.6% L- $\alpha$ -phosphatidic

acid(Sigma) were mixed with n-octyl- $\beta$ -o-glucopyranoside ( $\beta$ -OG, Anatrace) to a final detergent/phospholipid mass ratio of 1.1 in the solution of 100 mmol/L potassium phosphate, 0.2 mmol/L EDTA, and 1 mmol/L PMSF (pH 7.6). Final phospholipids concentration was approximately 40 g/L. This solution was further sonicated for 20 min. 100  $\mu\text{g}$  of rUCP1 were incubated and agitated in 1 ml of the sonicated solution for 30 min. Then 80 mg of SM-2 Bio-Beads (Bio-Rad), pretreated as described in Holloway *et al.*<sup>[20]</sup>, were added to absorb the detergent by 45 min agitation and this step was repeated 3 times every 45 min. Eventually, 150 mg of SM-2 Bio-Beads were added to remove detergent completely by shaking the solution gently overnight. All above incubation steps were performed at 4  $^\circ\text{C}$ . After detergent removal, liposome was formed and its external buffer was exchanged to 0.5 mmol/L Hepes, 0.2 mmol/L EDTA, and 0.28 mol/L sucrose (pH 7.3) by gel-filtration using Sephadex G25 (GE Healthcare).

For proton translocation activity assay, 100  $\mu\text{l}$  of above liposome was added to the 700  $\mu\text{l}$  solution containing 0.28 mol/L sucrose, 0.5 mmol/L Hepes (pH 6.8), 0.2 mmol/L EDTA, 1  $\mu\text{mol/L}$  Pyranine (Invitrogen) and 125  $\mu\text{mol/L}$  lauric acid (Acros). Then valinomycin (Val, Sigma) was added to final concentration 2.5  $\mu\text{mol/L}$ , initiating the proton translocation. The proton translocation was monitored by pyranine fluorescence (excitation wavelength 467 nm and emission wavelength 510 nm) that responses to the external buffer pH change, using the fluorescence-meter (Hitachi F-4500). The uncoupler carbonylcyanide m-chlorophenylhydrazone (CCCP, Sigma) was added to final concentration 2.5  $\mu\text{mol/L}$  as a positive control. The liposome without rUCP1 reconstituted in was used as negative control. And the proton translocation activity of reconstituted rUCP1-containing liposome was calculated by supposing CCCP could induce 100% potential proton transported from outside. All fluorescence measurements were repeated 3 times and averaged.

## 2 Results and discussion

### 2.1 rUCP1 expression could inhibit host growth

rUCP1 was cloned and inserted into vector pET22b and transformed into *E. coli* C41(DE3) strain. IPTG was used to induce rUCP1 expression. Empty vector pET22b and recombinant vector pET22b-LspA were transformed into the same strain as control.

Lipoprotein signal peptidase (LspA) is a bacterial lipoprotein-processing enzyme that cleaves the signal sequence from prolipoproteins after they are secreted and lipid-modified in the cell wall<sup>[21]</sup>. Comparing the growth curves of *E. coli* with and without rUCP1 or LspA expression (Figure 1), we found rUCP1 or LspA expression will inhibit the growth of host. As we know, as a native membrane protein of *E. coli*, LspA was expressed well and located in the plasma membrane. Induced expression of LspA inhibited the growth of bacteria indicated that over-expression of membrane proteins in *E. coli* would influence the host growth negatively. However, we found rUCP1 expression has more obvious inhibition effect than LspA expression, which indicated the expressed rUCP1 not only were located on the plasma membrane but also were in functional active state as proton translocators. At the same time, we found there were lots of *E. coli* autolysis occurred in the culture, which further indicated expressed rUCP1 was toxic to the host and induced cell membrane corruption.

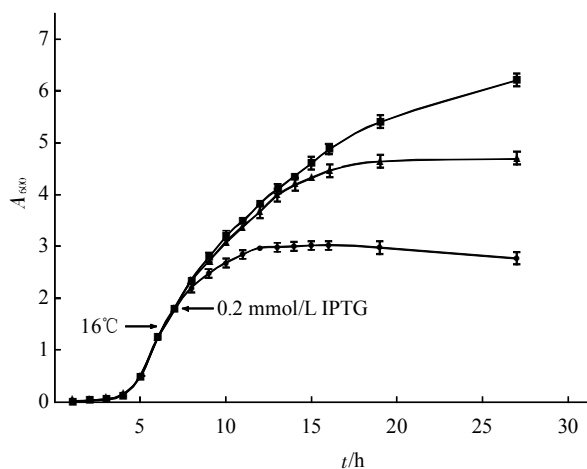


**Fig. 1 The growth curve of C41 with UCPI**

The solid square curve (■—■) is the control, C41 (DE3) strain transformed with empty pET22b plasmid. Another two are the curves of C41 (DE3) strain transformed with pET22b-rUCP1 plasmid (●—●) and pET22b-LspA plasmid (▲—▲). The x-axis is the time scale and the y-axis the optical density of culture at 600 nm. 0.2 mmol/L IPTG was added to induce protein expression. Error bars indicate s.e.m. ( $n=4$ ).

## 2.2 rUCP1 was overexpressed and purified by chromatography

rUCP1 gene was cloned into pET22b vector and the recombinant rUCP1 protein has the C-terminal fusion His-tag. The expression level of rUCP1 was

determined by Western blotting experiments using the anti-His antibody (Figure 2a). rUCP1 expression was tightly induced by IPTG and was found abundant in the extracted membrane after ultra-centrifugation that revealed expressed rUCP1 was located on the *E. coli* membrane and was further confirmed by immunoelectron microscopy below. Instead of Triton X-114<sup>[13]</sup> or Triton X-100<sup>[11]</sup>, LDAO was found to solubilize rUCP1 from cell membrane extraction effectively. Solubilized rUCP1 was further purified by Ni-NTA affinity column using C-terminal His-tag (Figure 2a and b) and gel filtration chromatography using Sephadex G25. For gel filtration, the LDAO-rUCP1 complex was eluted in the second peak and separated from large aggregation in the first peak (Figure 2c). The purified rUCP1 was finally concentrated to 4 g/L with the purity ~70%. The concentrated sample was not stable enough and easy to be precipitated, so the purified rUCP1 was quickly frozen in liquid nitrogen for future usage.

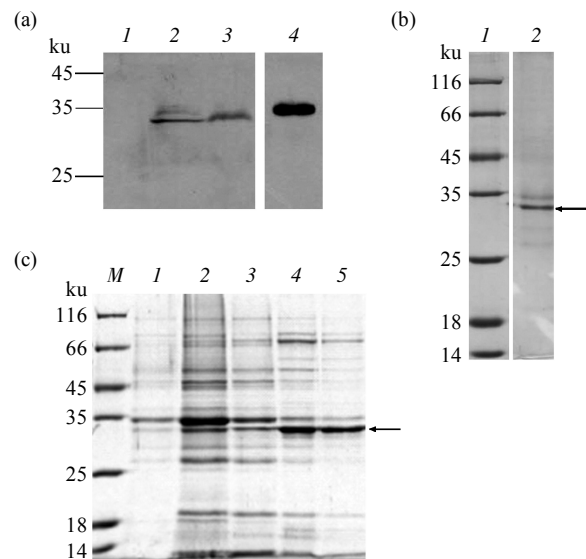


**Fig. 2 Expression and purification of rUCP1**

(a) The expression of rUCP1 detected by Western blots using the Anti-His antibody. The expression of rUCP1 was detected after IPTG induction and located on the supernatant of sonication lysed *E. coli* and purified by Ni-NTA affinity column. 1: Before induction; 2: After induction; 3: Supernatant after sonication; 4: UCPI eluted from Ni-NTA. (b) SDS-PAGE of rUCP1 that was purified by Ni-NTA affinity column. rUCP1 was eluted by 200 mmol/L imidazole and indicated by black arrow. Gel was stained with Coomassie blue R250. 1: Marker; 2: Elution. (c) SDS-PAGE of rUCP1 chromatography purification by Sephadex G25. M: Molecular mass marker; 1~3: The first elution peak; 4, 5: The second elution peak. Black arrow indicates the purified and concentrated rUCP1 that was proved by Western blotting (data not shown). Gel was stained with Coomassie blue R250.

### 2.3 Heterogeneously expressed rUCP1 was located on the bacterial membrane dominantly

In order to prove the heterogeneously expressed rUCP1 is functionally active, we examined its location in *E. coli* by immuno-labeling electron microscopy. There were few gold particles found in the immuno-labeled ultra-thin section of controlled *E. coli* without rUCP1 expressed (Figure 3a). However, for the immuno-labeled ultra-thin section of *E. coli* strain with rUCP1 expressed, lots of gold particles were found located on the membrane area and several particles were also located in the cytoplasm region (Figure 3b), which revealed most heterogeneously expressed rUCP1 were correctly located on the membrane and had the functional active form.

To further investigate the significance of expressed rUCP1 membrane localization, we explored the stereology counting method as described by Mayhew *et al*<sup>[22]</sup>. Briefly, 15 electron micrographs were selected randomly from different ultra-thin sections and proper square lattice was superposed into each micrograph. Then the gold particles or the lattice intersecting points located in the different regions (membrane, cytoplasm and whole micrograph) were counted and summarized respectively (Figure 3b and Table 1). Labeling density ( $LD$ ) in each region was calculated by  $LD = \text{number of observed gold particles } (N_{\text{obs}}) / \text{number of counted intersecting points } (P)$ . And the number of expected gold particles ( $N_{\text{exp}}$ ) in each region was calculated as  $P$  times the labeling density of whole micrograph ( $LD_{\text{total}}$ ). The relative labeling index

(RLI) in each region was determined by  $RLI = N_{\text{obs}} / N_{\text{exp}}$  and the *chi* square test by  $Chi = (N_{\text{obs}} - N_{\text{exp}})^2 / N_{\text{exp}}$ . The counting results and above parameters were calculated and listed in Table 1. Obviously, the relative labeling index for gold on membrane area is much larger than 1, indicating significant membrane localization propensity. *Chi* square test that *Chi* is much larger than 5.99 (in this test, the degree of system freedom,  $df$ , equals 2 for some gold particles are disperse outside cells) further supports the above conclusion. So it is quite obvious that gold particles are mainly located on the membrane, *i.e.* most of the rUCP1 were expressed and localized on the host membrane.

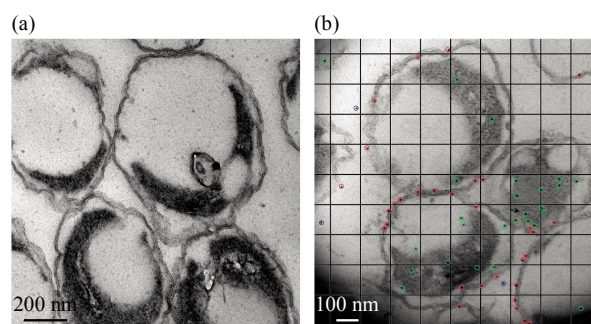


**Fig. 3 Electron microscopy of immuno-labeled rUCP1**

(a) Electron micrograph of ultra-thin section of *E. coli* transformed with empty pET22b plasmid. (b) Electron micrograph of ultra-thin section of *E. coli* transformed with pET22b-rUCP1 plasmid and expressing rUCP1. Red circles indicate the golds around membrane area, green circles for the golds in cytoplasm and blue circles for the region outside cell. The black lattice was randomly superposed into the electron micrograph. The diameter of colloid gold particles is about 10 nm and the scale bar is 100 nm.

**Table 1 Results of immuno-labeling scored by *chi* square test\***

	Observed golds ( $N_{\text{obs}}$ )	Observed points ( $P$ )	Labeling density ( $LD$ )	Expected golds ( $N_{\text{exp}}$ )	RLI ( $N_{\text{obs}}/N_{\text{exp}}$ )**	<i>Chi</i> square**
Membrane <sup>1)</sup>	156	88	1.77	43.6	3.58	290
Cytoplasm <sup>2)</sup>	131	292	0.450	144	0.910	1.17
Total <sup>3)</sup>	326	658	0.495			291.2

\* For the terminology explanation of each parameter, see the text (**Results and discussion**); \*\* When  $RLI > 1$  and *chi* square ( $df = 2, 0.05$ ) > 5.99, the localization conclusion is significantly obvious; <sup>1)</sup> Counting colloidal gold particles or lattice points that are located around cell membrane area (acceptance zone:  $\pm 15$  nm); <sup>2)</sup> Counting colloidal gold particles or lattice points that are located in the cytoplasm region; <sup>3)</sup> Counting whole colloidal gold particles or lattice points that are found in each electron micrograph.

### 2.4 Proton translocation activity of rUCP1

To further investigate the biological proton translocation activity of recombinant rUCP1, the purified rUCP1 was reconstituted into proteoliposome and its induced proton flux was examined by pyranine

fluorescence (Figure 4). The liposome without rUCP1 reconstituted did not show any proton uptake signal when Val was added. And the proteoliposome with rUCP1 reconstituted could translocate 20% proton from outside within 125 s, supposing CCCP could

induce 100% potential proton transported from outside. This experiment indicated the purified recombinant rUCPI owned the correct fold and exhibited functional proton translocation activity *in vitro*. Compared with CCCP, the relative low activity of rUCPI might be due to the low protein abundance reconstituted into proteoliposomes.

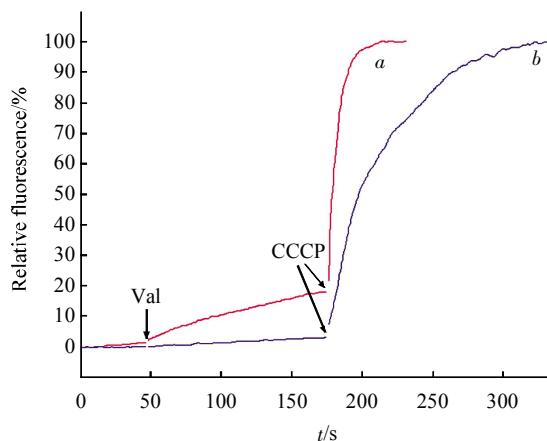


**Fig. 4 Proton translocation activity assay of rUCPI**

Trace *a*, proteoliposome with rUCPI reconstituted; Valinomycin (Val) was added at 50th second and carbonylcyanide *m*-chlorophenylhydrazine (CCCP) was added at 175th second. Trace *b*, liposome without rUCPI reconstituted as negative control. The *x*-axis is time scale and the *y*-axis is relative fluorescence scale.

In conclusion, this work firstly expressed functional active rat mitochondrial uncoupling protein 1 (rUCPI) by prokaryotic expression system. The expressed rUCPI could be toxic and inhibit host growth. Immuno-labeling electron microscopy and stereology counting quantification, as well as the fact rUCPI was extracted from the bacterial membrane, proved the heterogeneously expressed rUCPI was significantly localized on the host membrane. Purified rUCPI exhibited clear proton translocation activity when it was reconstituted into proteoliposome. The recombinant rUCPI could be expressed and purified in large-scale and used for further structural study.

**Acknowledgements** We would like to thank OUYANG Zhu-Qing for technical assistance.

### References

- [1] Echtay K S. Mitochondrial uncoupling proteins—what is their physiological role?. *Free Radic Biol Med*, 2007, **43** (10): 1351–1371
- [2] Krauss S, Zhang C Y, Lowell B B. The mitochondrial uncoupling protein homologues. *Nat Rev Mol Cell Biol*, 2005, **6**(3): 248–261
- [3] Cannon B, Nedergaard J. Brown adipose tissue: function and physiological significance. *Physiol Rev*, 2004, **84**(1): 277–359
- [4] Modriansky M, Murdza-Inglis D L, Patel H V, *et al.* Identification by site-directed mutagenesis of three arginines in uncoupling protein that are essential for nucleotide binding and inhibition. *J Biol Chem*, 1997, **272**(40): 24759–24762
- [5] Ledesma A, de Lacoba M G, Rial E. The mitochondrial uncoupling proteins. *Genome Biol*, 2002, **3**(12): REVIEWS3015
- [6] Klingenberg M, Huang S G. Structure and function of the uncoupling protein from brown adipose tissue. *Biochim Biophys Acta*, 1999, **1415**(2): 271–296
- [7] Garlid K D, Jaburek M, Jezek P. The mechanism of proton transport mediated by mitochondrial uncoupling proteins. *FEBS Lett*, 1998, **438**(1–2): 10–14
- [8] Jezek P, Orosz D E, Modriansky M, *et al.* Transport of anions and protons by the mitochondrial uncoupling protein and its regulation by nucleotides and fatty acids. A new look at old hypotheses. *J Biol Chem*, 1994, **269**(42): 26184–26190
- [9] Miroux B, Frossard V, Raimbault S, *et al.* The topology of the brown adipose tissue mitochondrial uncoupling protein determined with antibodies against its antigenic sites revealed by a library of fusion proteins. *Embo J*, 1993, **12**(10): 3739–3745
- [10] Pebay-Peyroula E, Dahout-Gonzalez C, Kahn R, *et al.* Structure of mitochondrial ADP/ATP carrier in complex with carboxyatractyloside. *Nature*, 2003, **426**(6962): 39–44
- [11] Lin C S, Klingenberg M. Isolation of the uncoupling protein from brown adipose tissue mitochondria. *FEBS Lett*, 1980, **113** (2): 299–303
- [12] Lin C S, Klingenberg M. Characteristics of the isolated purine nucleotide binding protein from brown fat mitochondria. *Biochemistry*, 1982, **21**(12): 2950–2956
- [13] Jaburek M, Garlid K D. Reconstitution of recombinant uncoupling proteins: UCPI, -2, and -3 have similar affinities for ATP and are unaffected by coenzyme Q10. *J Biol Chem*, 2003, **278** (28): 25825–25831
- [14] Hagen T, Zhang C Y, Vianna C R, *et al.* Uncoupling proteins 1 and 3 are regulated differently. *Biochemistry*, 2000, **39**(19): 5845–5851
- [15] Zhang C Y, Hagen T, Mootha V K, *et al.* Assessment of uncoupling activity of uncoupling protein 3 using a yeast heterologous expression system. *FEBS Lett*, 1999, **449**(2–3): 129–134
- [16] Tartof K D, Hobbs C A. Improved media for growing plasmid and cosmid clones. *Focus*, 1987, **9**: 12
- [17] Sakae Y, Yasuda Y, Tochikubo K. Immunoelectron microscopic localization of one of the spore germination proteins, GerAB, in *Bacillus subtilis* spores. *J Bacteriol*, 1995, **177**(21): 6294–6296
- [18] Echtay K S, Winkler E, Frischmuth K, *et al.* Uncoupling proteins 2 and 3 are highly active H(+) transporters and highly nucleotide sensitive when activated by coenzyme Q (ubiquinone). *Proc Natl Acad Sci USA*, 2001, **98**(4): 1416–1421
- [19] Rigaud J L, Levy D. Reconstitution of membrane proteins into liposomes. *Methods Enzymol*, 2003, **372**: 65–86

- [20] Holloway P W. A simple procedure for removal of Triton X-100 from protein samples. *Anal Biochem*, 1973, **53**(1): 304-308
- [21] Sankaran K, Wu H C. Lipid modification of bacterial prolipoprotein. Transfer of diacylglycerol moiety from phosphatidylglycerol. *J Biol Chem*, 1994, **269**: 19701-19706
- [22] Mayhew T M, Griffiths G, Lucocq J M. Applications of an efficient method for comparing immunogold labelling patterns in the same sets of compartments in different groups of cells. *Histochem Cell Biol*, 2004, **122**(2): 171-177

## 线粒体内膜解偶联蛋白 UCP1 在大肠杆菌中的活性表达\*

周强军 孙 吉 翟宇佳 孙 飞\*\*

(中国科学院生物物理研究所, 生物大分子国家重点实验室, 北京 100101)

**摘要** 线粒体的呼吸耗氧偶联着 ATP 的合成, 而位于线粒体内膜上的跨膜蛋白解偶联蛋白(uncoupling protein, UCP)能够破坏这种偶联关系. 在大肠杆菌中表达了有生物活性的鼠源解偶联蛋白 1(rUCP1). 重组 rUCP1 的表达导致大肠杆菌宿主细胞生长变慢; 在电子显微镜下观察免疫标记的结果显示, 重组 rUCP1 主要表达在细菌膜上; 同时将 rUCP1 重构到脂质体中也能测到质子转运活性. 这些结果说明, 真核生物 UCP1 能够在原核生物中表达出有生物活性的形式, 且能纯化得到足量的 rUCP1 蛋白用于进一步的结构生物学研究.

**关键词** 线粒体解偶联蛋白, 原核表达, 免疫电镜, 膜蛋白, 脂质体

**学科分类号** Q71

**DOI:** 10.3724/SP.J.1206.2009.00531

\* 国家重点基础研究发展计划(973)(2006CB503910, 2006CB806506, 2006CB911001) 和国家自然科学基金(30721003)资助项目.

\*\* 通讯联系人.

Tel/Fax: 010-64888582, E-mail: feisun@ibp.ac.cn

收稿日期: 2009-09-10, 接受日期: 2009-12-01